Removal of CO$_2$ from Natural gas stream using Silica Membrane

By

Nas Aaryu Bin Hussein

Dissertation submitted in partial fulfillment of

the requirement for the

Bachelor of Engineering (Hons)

(Chemical Engineering)

JANUARY 2009

Universiti Teknologi PETRONAS

Bandar Seri Iskandar

31750 Tronoh
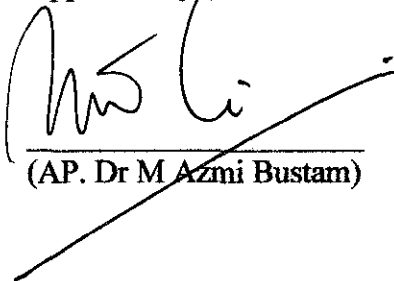
Perak Darul Ridzuan

CERTIFICATION OF APPROVAL

Removal of CO$_2$ from Natural gas stream using

Silica Membrane

By

Nas Aaryu Bin Hussein

A project dissertation submitted to the

Chemical Engineering Programme

Universiti Teknologi PETRONAS

in partial fulfilment of the requirement for the

BACHELOR OF ENGINEERING (Hons)

(CHEMICAL ENGINEERING)

Approved by

_____

(AP. Dr M Azmi Bustam)

UNIVERSITI TEKNOLOGI PETRONAS

TRONOH, PERAK

January 2009

CERTIFICATION OF ORIGINALITY

This is to certify that I am responsible for the work submitted in this project, that the original work is my own except as specified in the references and acknowledgements, and that the original work contained herein have not been undertaken or done by unspecified sources or persons.

_____

NAS AARYU BIN HUSSEIN

ABSTRACT

In this study the synthesis, characterization, and gas transport properties of silica membranes supported on porous alumina substrate in separating or removing carbon dioxide (CO_2) from natural gas stream (CH_4) were studied. Silica membranes are prepared by dip-coating a prepared porous alumina support in a polymeric silica sol made by base-catalyzed hydrolysis and condensation of tetraethyl orthosilicate (TEOS), $Si(OCH_2CH_3)_4$, in ethanol.

The membranes were characterized using Scanning Electron Microscopy and the single gas permeation test. From the SEM observation, silica membrane was tightly attached to the substrate and the average thickness of the membrane was approximately 15-16 μm. The effect of dipping time during dip-coating of the porous alumina support also been studied. Longer dipping time may improve the selectivity. Total of three samples have been produced with the same silica sol gel but at different dipping time which are at 1, 2 and 3 hour. The silica membranes with 3 hour of dipping time displayed high CO_2 permeance (3.35963×10^{-6} mol/m^2.s.Pa) but small selectivity of 1.398 towards CO_2. The gas permeation test is conducted at room temperature and with different feed pressure of 1.5, 2.0, 2.5 and 3.0 bar.

All synthesized silica membrane, show high permeance of CO_2 (CO_2 permeance > CH_4 permeance) thus give the evidence that the mechanism of molecular differentiation by silica layer is through size selectivity. However, the selectivity of these membranes is smaller compared to idea Knudsen separation factor of 1.66. This small deviation from ideal Knudsen diffusion may be due to a minute number of microcracks in the membrane layer, which were not observable by SEM, but detected by this test. (Small defects and cracks often appear in thin films during the calcinations process).However, the selectivity of the synthesized silica membrane can be improved through some modification which is by applying multiple separation layer of silica sol on the top membrane. The formation of several separation layers will gradually decreased the pore size of the membrane leading to greater selectivity of separation gas especially CO_2 and CH_4 separation.

ACKNOWLEDGEMENT

TABLE OF CONTENT

CHAPTER 4: RESULT AND DISCUSSION

CHAPTER 5: CONCLUSION AND RECOMMENDATION

APPENDIX

LIST OF FIGURES

Figure 1.1 Differences in molecular size of gases

Figure 2.1: Reaction take place in sol-gel process

Figure 2.2: Acid-Catalyzed Hydrolysis

Figure 2.3: Base-Catalyzed Hydrolysis

Figure 2.4: Nucleophilic Attack to Form Siloxane Bond

Figure 2.5: Summary of Acid/Base Sol-Gel Conditions

Figure.2.6: SEM micrograph of a Si(400) membrane cross section showing a part of the γ-Al_2O_3 layer and the silica layer at high magnification (a) and the α-Al_2O_3 support and g γ-Al_2O_3 layers at lower magnification (b).

Figure 2.7: Temperature dependence of the permeance for the Si(400) membranes at P=1 bar

Figure 2.8 :(a) Permeance of single-step membrane to various gases, (b) Comparison of permeance of Single and two step membrane to CO_2 as a function of temperature

Figure 3.1: (a) Extrusion die and hand press used in Extrusion of Alumina powder to from porous alumina disc. (b) Furnace used in sintering process and (c) Sintered porous alumina membrane support

LIST OF TABLES

CHAPTER 1

INTRODUCTION

1.1 Background of the Study

The separation of CO_2 from CH_4 is important in natural gas processing because CO_2 reduces energy content of natural gas. Also, CO_2 is acidic and corrosive in the presence of water within the transportation pipeline and/or storage system. About 17% of natural gas in United States is treated to remove CO_2 before it is passed to the pipeline [1]. Pipeline specifications for natural gas require a CO_2 concentration below 2–3% [2] .The technology most widely used for CO_2 removal is amine adsorption, but amine plants are complex and costly [1]. Membrane plants using CO_2-selective cellulose acetate membranes were installed since 1980s and the using this method reduce the percentage of CO_2 from 36% at the inlet to product specification of less than 16% CO_2 [2]. However this technique has several drawbacks. The main problems that limit the use of polymeric membranes are their poor performance stability at high pressure and in the presence of highly sorbing components [3]. In some cases, high CO_2 partial pressures plasticize polymer membranes, and thus decrease their separation ability [3].
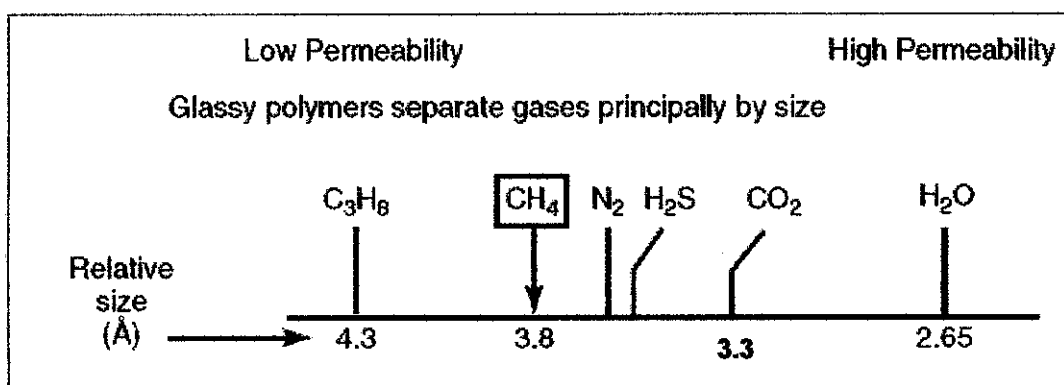
Figure 1.1 Differences in molecular size of gases

1.2 Problem Statement

In order to minimize those effects that being stated in introduction section earlier, and to achieve a CO_2 concentration below 2–3% in pipeline[2] a good separation unit that give lower cost and can stand harsh condition should be establish. There two method used in industry in removing CO_2 from natural gas stream, which are amine adsorption plant and membrane (polymeric or ceramic membrane).

However, due to those constraint offered by amine plant and polymeric membrane in removing CO_2 from natural gas stream, a microporous inorganic (ceramic) membrane that separate base on different molecular size of gases should be use for the separation of CO_2 from CH_4.

1.3 Objective and Scope of Study

This research focused on the development of microporous ceramic membrane which is Silica Membrane for the removal of Carbon Dioxide (CO_2) from Natural gas (CH_4) stream. The objectives of this research project are:

- To study and demonstrate the separation of carbon dioxide(CO_2) from natural gas stream using microporous ceramic membrane technology
- To evaluate the performance of silica membrane in term of CO_2 and CH_4 permeance as well as CO_2/CH_4 ideal selectivity.
- To study the effect of dipping time on the performance of silica membrane in term of CO_2 and CH_4 permeance as well as CO_2/CH_4 ideal selectivity.

The scopes of study in this project are first to performed literature review on the best technique in synthesizing the desired Silica Membrane. Then the synthesized Silica membrane will be characterizes and further tested. In chapter 3 and 4, the synthesis, characterizations and gas permeation result for CO_2 and CH_4 on Silica membrane supported on porous alumina, are presented.

CHAPTER 2
LITERATURE REVIEW / THEORY

2.1 Ceramic Membrane for gas separation

There are two types of ceramic membranes suitable for gas separations which are dense and porous, especially microporous membranes. Dense Ceramic Membranes are made from crystalline ceramic materials such as fluorites, which allow permeation of only oxygen or hydrogen through the crystal lattice. Therefore, they are mostly impermeable to all other gases, giving extremely high selectivity towards oxygen or hydrogen. They are mainly composed of amorphous silica or zeolites. They are usually prepared as a thin film supported on a macroporous ceramic support, which provides mechanical strength, but offers minimal gas transfer resistances. In most cases, some intermediate layers are required between the macroporous support and the top separation layer to bridge the gap between the large pores of the support and the small pores of the top separation layer. This paper will focus on Microporous Ceramic Membrane prior to the separation of CO_2 from CH_4.

2.2 Microporous Ceramic Membranes

There are two main types of microporous membranes used in gas separations, namely crystalline zeolite membranes and amorphous membranes such as silica and carbon membrane. The practically useful crystalline microporous membranes have polycrystalline structures, consisting of many crystallites packed together without any crystallite (grain) boundary gap in the ideal case. These inorganic membranes with good thermal, chemical and mechanical stability have attracted considerable attention due to their potential applications in gas and vapor separations at elevated temperatures under harsh conditions [4]. Microporous inorganic membranes, such as Polycrystalline zeolite, amorphous carbon and sol–gel silica comprise a particularly important category of inorganic membranes, useful for a variety of separations including permanent gases or hydrocarbon isomers, based on differences in

diffusivities and/or adsorption strengths of mixture components in membrane pores [5].

2.2.1 Zeolite Membrane

Zeolite membranes made by direct or seeded hydrothermal growth on porous ceramic or metallic supports have attracted considerable attention during the last decade, on account of very exciting transport properties and the potential for a variety of separations including O_2/N_2 [6], CO_2/N_2 [7], linear/branched paraffins [8], C8 aromatics [9], saturated/unsaturated hydrocarbons [10] and water/alcohol mixtures [11]. Membranes of various zeolite such as SAPO-34, ZSM-5, Y-type, silicalite A-type and p-type have been synthesized on porous support for gas separation (Shekhawat, 2003). Zeolite membranes can be prepared by in situ hydrothermal synthesis in porous stainless steel, α-alumina, or γ-alumina disks for gas permeation studies. These supported zeolite membranes have a thin and continuing zeolite separation layer with the porous support providing mechanical strength to the membrane (Shekhawat, 2003).

Most of the current researches on the separation of CO_2 from CH_4 are carried out using Y-type and SAPO-34 membrane. Table 2.1 shows some of the reported result of permeation test based on Y-type and SAPO-34 materials.

4

Table 2.1 CO_2/CH_4 separation properties of Y-type and SAPO-34 membranes

Zeolite	Temperature (°C)	Permeance of CO_2	Selectivity of CO_2/CH_4	Reference
Y-type	30	352.94	2	Kusakabe et al., 1997
	80	882.35	4	
	130	882.35	6	
SAPO-34	27	441.17	16	Poshusta et al., 2000
	100	235.3	9	
	200	58.82	4	
SAPO-34	24	294.12	25	Li et al., 2004
	97	235.3	17	
	147	147.06	10	
	197	88.235	5	

2.2.2 Carbon Membrane

Carbon membranes are highly selective due to their pore of molecular dimension. They ar relatively inexpensive membranes and are prepared basically by carbonizing organic polymers as starting materials at high temperature under controlled condition. It is expected that carbonized materials are stable at high temperature and resist chemical attack. Carbon membranes prepared by pyrolysis of polymeric precursor films deposited on porous supports have shown potential for gas/vapor separations based on either size (e.g. CO_2/CH_4) or adsorption (e.g. H_2/hydrocarbons) differences of mixture components in membrane micropores [12, 13].

Despite their exciting transport properties, several technical problems may limit the usefulness of zeolite or carbon molecular sieve membranes for commercial applications. These include poor processibility and scaleability, low permeation fluxes due to large thicknesses, and compromised selectivities due to susceptibility to cracking or undesirable intercrystalline porosity.

However, Sol–gel derived silica membranes represent another class of microporous molecular sieve membranes that can offer considerable advantages compared to zeolite or carbon membranes.

2.2.3 Silica Membrane

Microporous silica (SiO_2) membranes are prominent representatives of amorphous membranes. The first successful silica membranes for gas permeation/separation with good quality and high flux were prepared in 1989 using a sol-gel method where SiO2 polymer sols were firstly prepared by acid catalysed hydrolysis of tetraethoxysilane (TEOS) in alcoholic solution.

This membranes are typically processed using a simple dip-coating step at ambient conditions, their thickness can be controlled easily in the range 20–100nm to improve permeation flux, and their pore size and porosity can be fine-tuned by the sol chemistry to obtain the desired separation function [14, 15].

Silica membranes are typically prepared by dip-coating a suitable support in a polymeric silica sol made by acid/base-catalyzed hydrolysis and condensation of tetraethyl orthosilicate (TEOS), $Si(OCH_2CH_3)_4$, in ethanol [16,17]. During deposition, preferential evaporation of ethanol results in the formation of a xerogel film on the surface of the support, via interpenetration and collapse of the fractal siliceous clusters contained in the sol, whereas water molecules trapped between neighbouring clusters result in the formation of micropores in the size range 3–4Å, after complete drying.

2.3 Sol Gel Process

Sols are dispersions of colloidal particles (size 1 - 100 nm) [18] in a liquid. The sol-gel process, as the name implies, involves the evolution of inorganic networks through the formation of a colloidal suspension (sol) and gelation of the sol to form a network in a continuous liquid phase (gel).The precursors for synthesizing these colloids consist of a metal or metalloid element surrounded by various reactive ligands. Metal alkoxides are most popular because they react readily with water. The most widely used metal alkoxides are the alkoxysilanes, such as tetramethoxysilane (TMOS) and tetraethoxysilane (TEOS).However, other alkoxides such as aluminates, titanates, and borates are also commonly used in the sol-gel process, often mixed with TEOS.

At the functional group level, three reactions are generally used to describe the sol-gel process: **hydrolysis, alcohol condensation, and water condensation.** This general reaction scheme can be seen in Figure 2.1. However, the characteristics and properties of a particular sol-gel inorganic network are related to a number of factors that affect the rate of hydrolysis and condensation reactions, such as, pH, temperature and time of reaction, reagent concentrations, catalyst nature and concentration, H_2O/Si molar ratio (R), aging temperature and time, and drying.
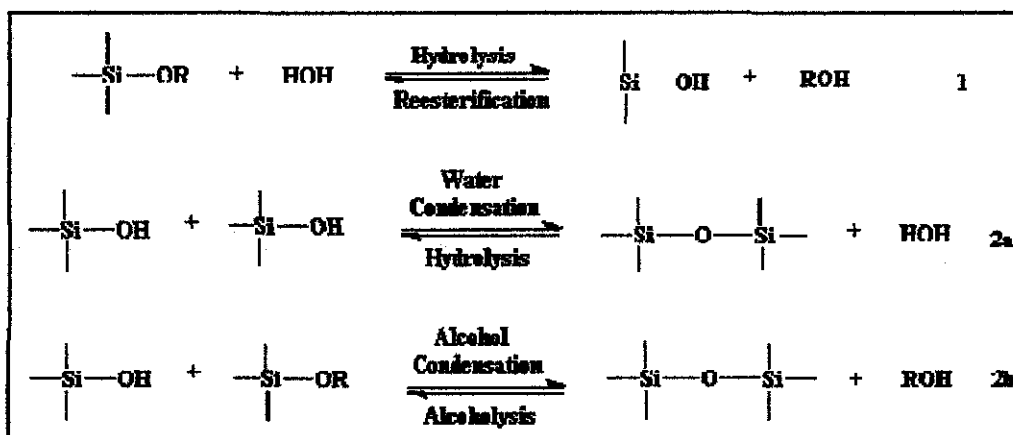
Figure 2.1.Reaction mechanism take place in sol-gel process

2.3.1 Hydrolysis

Hydrolysis can occur without addition of an external catalyst, but it is most rapid and complete when they are employed. This hydrolysis process can occur under acid or basic condition. Mineral acids (HCl) and ammonia are most generally used.

However, other catalysts are acetic acid, KOH, amines, KF, and HF. Additionally, it has been observed that the rate and extent of the hydrolysis reaction is most influenced by the strength and concentration of the acid- or base catalyst.

Under basic conditions, the hydrolysis reaction was found to be first-order in base concentration. However, as the TEOS concentration was increased the reaction deviated from a simple first-order to a more complicated second-order reaction. With weaker bases such as, ammonium hydroxide and pyridine, measurable speeds of reaction were produced only if large concentrations were present. Therefore, compared to acidic conditions, base hydrolysis kinetics is more strongly affected by the nature of the solvent.

2.3.1.1 Acid-Catalyzed Hydrolysis Mechanism

Under acidic conditions, it is likely that an alkoxide group is protonated in a rapid first step. Electron density is withdrawn from the silicon atom, making it more electrophilic and thus more susceptible to attack from water. This results in the formation of a penta-coordinate transition state with significant SN2-type character (SN2-type indicate a substitution, nucleophilic, bimolecular reaction mechanism) The transition state decays by displacement of an alcohol and inversion of the silicon tetrahedron, as seen in Figure 2.2.
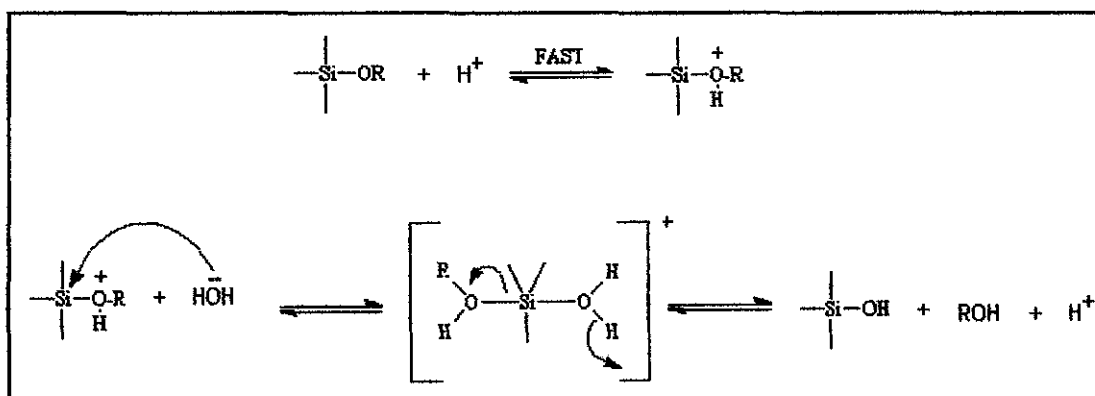
Figure 2.2; Acid-Catalyzed Hydrolysis

2.3.1.2 Based-Catalyzed Hydrolysis Mechanism

Base-catalyzed hydrolysis of silicon alkoxides proceeds much more slowly than acid-catalyzed hydrolysis at an equivalent catalyst concentration. Basic alkoxide oxygens tend to repel the nucleophile, -OH. However, once an initial hydrolysis has occurred, following reactions proceed stepwise, with each subsequent alkoxide group more easily removed from the monomer then the previous one. Therefore, more highly hydrolyzed silicones are more prone to attack. Additionally, hydrolysis of the forming polymer is more sterically hindered than the hydrolysis of a monomer. Although hydrolysis in alkaline environments is slow, it still tends to be complete

8

and irreversible. Thus, under basic conditions, it is likely that water dissociates to produce hydroxyl anions in a rapid first step. The hydroxyl anion then attacks the silicon atom. Again, an SN2-type mechanism has been proposed in which the -OH displaces -OR with inversion of the silicon tetrahedron. This is seen in Figure 2.3.
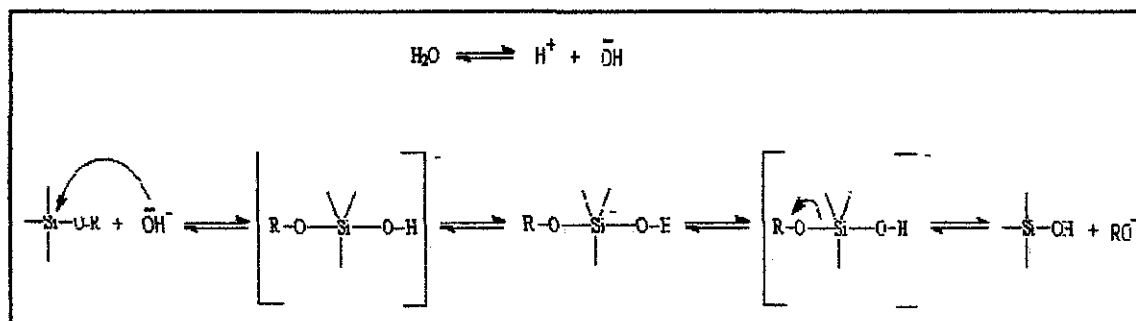
Figure 2.3; Base-Catalyzed Hydrolysis

As with hydrolysis, condensation can proceed without catalyst, however, their use in organosiloxanes is highly helpful. Furthermore, the same type catalysts are employed: generally those compounds which exhibit acidic or basic characteristics.

It has been shown that condensation reactions are acid and base specific. In addition, under more basic conditions, gel times are observed to increase. Condensation reactions continue to proceed; however, gelation does not occur. Again, catalysts which dictate a specific pH, can and do drive the type of silica particle produced as seen in the previous discussion on pH.

2.3.2 Condensation

2.3.2.1 Acid-Catalyzed Mechanism

It is generally believed that the acid-catalyzed condensation mechanism involves a protonated silanol species. Protonation of the silanol makes the silicon more electrophilic and thus susceptible to nucleophilic attack. The most basic silanol

species (silanols contained in monomers or weakly branched oligomers) are the most likely to be protonated. Therefore, condensation reactions may occur preferentially between neutral species and protonated silanols situated on monomers, end groups of chains.

2.3.2.2 Base-Catalyzed Mechanism

The most widely accepted mechanism for the base-catalyzed condensation reaction involves the attack of a nucleophilic deprotonated silanol on a neutral silicic acid: 25

Figure 2.4: Nucleophilic Attack to Form Siloxane Bond

As summary there are many factors affect the resulting silica network, such as, pH, temperature and time of reaction, reagent concentrations, catalyst nature and concentration, H_2O/Si molar ratio (R), aging temperature and time. However, it can generally be said that sol-gel derived silicon oxide networks, under acid-catalyzed conditions, yield primarily linear or randomly branched polymers which entangle and form additional branches resulting in gelation. On the other hand, silicon oxide networks derived under base-catalyzed conditions yield more highly branched clusters which do not interpenetrate prior to gelation and thus behave as discrete clusters (See Figure 2.5).
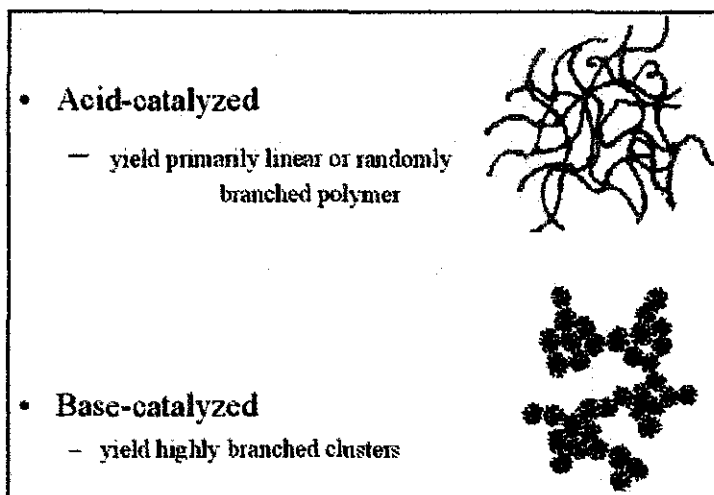
- Acid-catalyzed

  — yield primarily linear or randomly
    branched polymer

- Base-catalyzed

  — yield highly branched clusters

Figure 2.5: Summary of Acid/Base Sol-Gel Conditions

2.4 Mechanism of Gas Transport through a Supported Silica Membrane

There have been many studies associated with gas transport through membranes, and extensive discussions can be found in the literature [19-24]. A variety of models have been used to describe the transport through membranes such as porous glass [19,20], zeolites [21,23], alumina and silica [24]. These models have different theoretical bases associated with the details of the gas diffusion mechanism. Sorption and diffusion are two major process that play important roles in the overall gas transport, where sorption describes the interactions between gas molecules and the membrane surface, and diffusion describes the rate of gas passage through the membrane. Qualitative and quantitative analysis of the involvement of these steps is required to understand the overall gas transport mechanism since each process can contribute to the total permeation rate, and its importance will differ according to such variables as temperature, pressure, and composition.

Sorption of gas molecules from the bulk gaseous state to the surface of the membranes can occur physically or chemically depending on the nature of the force between the gas molecules and the surface. Chemisorption occurs when the interactions are strong, for example, in the dissociative adsorption of hydrogen molecules on palladium membranes [25].

11

Physisorption occurs when the interactions with the surface are weak, for example, in the adsorption of CO_2 on microporous glass membranes [26]. In the subsequent transport process the adsorbed molecules diffuse through the membrane in various ways under the driving force of a concentration gradient. Detailed discussion of these sorption and diffusion steps follows in the next sections

2.4.1 Theoretical Background

Fick's first law applies for the macroscopic description of transport process,

$$J = -D(c)\nabla c \quad \text{...................} (2.1)$$

Where J is the flux (mol m^{-2} s^{-1}), D(c) is the concentration dependent diffusivity (m^{2}s^{-1}), and c is the concentration (mol m^{-3}).

2.4.1.1 Sorption

Gas transport through microporous or dense materials such as zeolites or bulk solid oxides requires adsorption of molecules before the subsequent diffusion process. Numerous sorption models have been reported in the literature based on different assumptions about the state of the adsorbed gas [27]. In membrane applications for gas separation, adsorption is usually not multilayer, and often well below a monolayer, so is well described by the Langmuir adsorption model [28].

$$\theta = \frac{q}{q_s} = \frac{bP}{1 + bP} \quad \text{.........................} (2.2)$$

where q is the fractional occupancy of adsorption sites, q is the amount of adsorbed gas molecules per unit mass of adsorbent (mol g^{-1}), q_s is the saturation amount of adsorbed molecules, P is the pressure (Pa) and b is an equilibrium adsorption

constant (Pa⁻¹).The dependency of the equilibrium adsorption constant on temperature is given by,

$$b = b_0 \exp\left(\frac{\Delta H_a}{RT}\right)$$ ....(2.3)

Where ΔH_a is the heat of adsorption. At low pressure and high temperature (small values of b), the Langmuir equation may be simplified to,

$$q = q_s bP = KP = K_0 \exp\left(\frac{\Delta H_a}{RT}\right)(P)$$ ....(2.4)

Where K is a Henry's constant (mol g⁻¹ Pa⁻¹). In the Henry's law regime the amount of adsorbed molecules increases linearly with applied pressure.

2.4.1.2 Diffusion

Diffusion of molecules through a membrane can proceed in various ways depending on the nature of the interaction between the diffusing gas molecules and the membrane. Various gas diffusion processes were discussed by Burggraaf [21] in terms of the associated energy potential wells developed inside the pores of membrane. The shapes of these energy potential wells depend mainly on the distance between the pore walls and the diffusing gas molecules. Therefore, the ratio of the molecular size of the diffusing gas and the pore diameter plays a major role in determining which diffusion mechanism may apply. We will discuss four different gas diffusion mechanisms (Knudsen, gas translational (GT), solid state, and surface diffusion) that are often involved in gas transport through membranes.

Knudsen diffusion occurs when the mean free path of the diffusing gas molecules is much larger than the pore size [29]. In this regime the gas molecules pass through the pores undergoing random collisions with the pore walls, and the Knudsen

diffusivity is obtained from the gas kinetic velocity and the geometric parameters associated with the membrane.

$$D = \frac{\varepsilon d_p}{3\tau} \left(\frac{8RT}{\pi M}\right)^{\frac{1}{2}} \quad \ldots\ldots\ldots\ldots\ldots (2.5)$$

Where ε is the porosity of the membrane, d_p is the pore diameter, τ is the tortuosity, R is the gas constant and M is molecular weight of the diffusing gas.

The gas translational (GT) diffusion mechanism has been applied to microporous materials such as zeolites [21,23]. The expression obtained is similar to the Knudsen equation, but in this model the gas molecules are considered to move between sorption sites (cages) in a translational mode by overcoming the obstructions formed by the small channels that connect adjacent sorption sites. The GT diffusivity is given by,

$$D = g_d d_p \left(\frac{8RT}{\pi M}\right)^{\frac{1}{2}} \exp\left(-\frac{\Delta E}{RT}\right) \quad \ldots\ldots\ldots\ldots (2.6)$$

where g_d is a geometric factor, d_p is the pore size of the material and ΔE is the activation energy of diffusion. The activation energy is considered to be the difference between the potential energy in the sorption sites and in the channels of the zeolites.

As the ratio of the pore size of the membrane versus the size of the diffusing gas molecule decreases, the energy potential in the pores will develop into a steep parabolic potential where the movement of gas molecules changes from a translational to a vibrational mode. A bound molecule in one sorption site will jump to other sorption sites with a vibrational frequency, v_e and a jump length, λ.

In this regime the gas diffusion is similar to solid state diffusion, and the diffusivity is given by [21]:

$$D = g_d \lambda^2 v_e \exp\left(-\frac{\Delta E}{RT}\right)$$ .... (2.7)

Where g_d is a geometric constant and ΔE is the activation energy of diffusion. A model for solid state diffusion also can be obtained by a statistical approach. For gas diffusion in fused silica glass, a statistical model of monatomic gas diffusivity is given by [30]:

$$D = \frac{1}{6}\left(\frac{kT}{h}\right)d^2\left(\frac{\left(e^{hv/2kT} - e^{-hv/2kT}\right)^3}{\left(e^{hv'/2kT} - e^{-hv'/2kT}\right)^2}\right)e^{-\Delta E/RT}$$ .... (2.8)

where k is Boltzmann's constant, h is Planck's constant, d is the distance between sorption sites in the structure, T is the absolute temperature, n is the vibrational frequency of gas molecules on the sorption sites, n* is the vibrational frequency on the doorway sites, R is the gas constant, and ΔE is the activation energy of diffusion. Surface diffusion can be expressed in the same way as solid state diffusion except that the model equation obtained has a 2-dimensional physical meaning. In surface diffusion gas molecules are considered to be adsorbed on the surface and to move on the surface by hopping between the potential minima produced on the pore surface [21]. However, the diffusing gas molecules bound on the surface may escape from their adsorbed state to the gaseous state if their kinetic energy is larger than their sorption energy. Thus, surface diffusion is only applicable in a relatively low temperature range that depends on the sorption energy of the gas molecules. Also, the activation energy for surface diffusion is lower than the sorption energy.

2.4.1.3 Permeation

The flux (mol $m^{-2}s^{-1}$) of gas transport through the membranes is obtained using Fick's first law. In gas phase membrane applications permeance and permeability are

15

usually used as measures of gas transport rate. The permeance, Q, (mol m^{-2} s^{-1} Pa^{-1}) is defined as the flux per unit pressure difference between the two sides of the membrane. If the thickness of the separation layer of the membranes is known, the permeability coefficient, P, (mol m^{-1} s^{-1}Pa^{-1}) is obtained by normalizing the permeance by the unit thickness of the separation layer.

Gas transport by Knudsen diffusion occurs in the gaseous state without involvement of adsorption. Therefore, the molar flux (molm^{-2}s^{-1}) can be obtained using the Knudsen diffusivity and Fick's first law, where the concentration is obtained using the ideal gas law. The Knudsen permeance is then given by,

$$Q = \frac{\varepsilon \, d_p}{\tau L}\left(\frac{8}{9\pi M RT}\right)^{\frac{1}{2}} \quad \text{................(2.9)}$$

Where L is the thickness of the membrane.

In many cases of gas permeation through microporous membranes, gas molecules adsorb on the membranes. This adsorption is followed by diffusion to the opposite side of the membranes where the molecules desorb to the gaseous state. In Henry's law regime the amount of adsorption on the membrane is linearly proportional to the partial pressure (Eq. 2.4). Therefore, the permeance is obtained using the diffusivity and Henry's constant (K).

$$Q = \frac{\rho \, \varepsilon}{L} D_0(q) \, K_0 \exp\left(\frac{\Delta H_a}{RT}\right)\exp\left(\frac{-\Delta E}{RT}\right) = Q_0 \exp\left(\frac{\Delta H_a - \Delta E}{RT}\right) \quad \text{.........(2.10)}$$

Where r is the density of the membrane (g m^{-3}).

There also have been a few statistical studies describing adsorption and diffusion of gas molecules through vitreous silica glass [30-32]. The solubility (mol m^{-3} Pa^{-1}), S, of small gases in the silica glass is given by [32]:

$$S = \frac{n_x}{N_A P} = \left(\frac{h^2}{2\pi m k T}\right)^{\frac{3}{2}} (k T)^{-1} \frac{N_S}{N_A} \left(\frac{e^{-hv/2kT}}{1 - e^{-hv/kT}}\right)^3 e^{E(0)/RT} \quad \ldots\ldots\ldots (2.11)$$

where n_s is the number of gas molecules dissolved per m^3 of glass volume, P is the applied gas pressure, m is the mass of the molecule, h is Planck's constant, k is Boltzmann's constant, n is the vibrational frequency of gas molecules on the sorption sites, T is temperature, N_s is the number of solubility sites available per m3 of glass volume, NA is Avogadro's number, R is the gas constant, and E(0) is the binding energy of the physically dissolved gas molecule in an interstitial sorption site. The permeability, P, of a monatomic gas through silica glass is obtained by using the solubility equation (Eq. 2.11) and the diffusivity equation (Eq. 2.8), and the permeance is obtained by including the thickness of the separation layer, L, in the permeability equation [30].

$$Q = \frac{1}{6L}\left(\frac{d^2}{h}\right)\left(\frac{h^2}{2\pi m k T}\right)^{\frac{3}{2}} \frac{(N_S/N_A)}{(e^{hv'/2kT} - e^{-hv'/2kT})^2} e^{-\Delta E_k/RT} \quad \ldots\ldots\ldots (2.12)$$

Where the ΔE_k is the activation energy for the permeation. In the case of polyatomic molecules rotational partition functions on the solubility site and sorption site are also considered in the model equation.

2.5 Previous and Current Development of Silica Membrane

2.5.1 By Renate M. de Vos, Henk Verweij *

Silica membranes with extremely low defect concentrations have been prepared using sol–gel synthesis starting from tetraethyl orthosilicate (TEOS).Two type of membrane have produced that only differ in their sintering temperature noted as "Si(400)" and "Si(600)" for sintering temperature of 400°C and 600°C respectively. An asymmetric structure is obtained by applying two silica layers on top of a γ-Al_2O_3 layer, supported by a α-Al_2O_3 support. The selective silica top layers have a total

thickness of 30 nm and micropores with a pore diameter ~5Å, determined by physical adsorption on unsupported silica membrane material. The transport properties of the membranes are measured in the temperature range of 50–300°C and at pressure differences ranging from 0.5 to 3 bar. The membranes have reproducible high permeances (2×10^{-6}mol/m^{2}s Pa) for H_2 and much lower permeances for CO_2, N_2, and O_2 (~10 x lower), CH_4 (~500 x lower).

2.5.1.1 Membrane Characterization

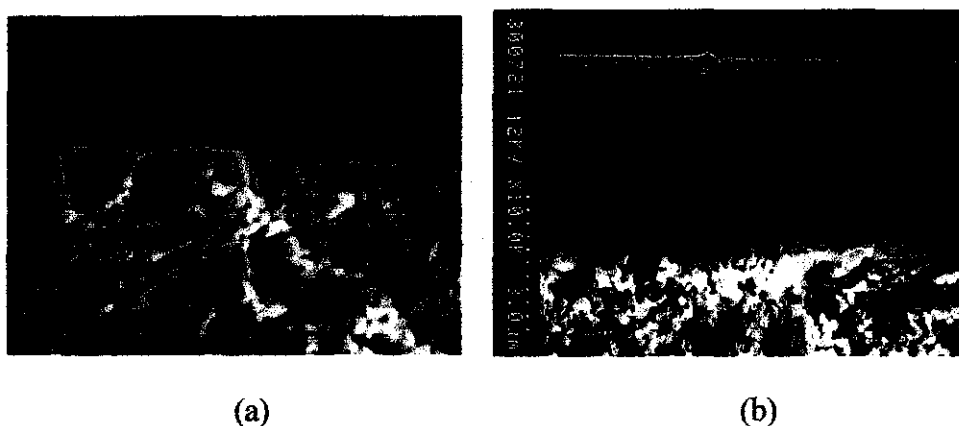(a)   (b)

Fig.2.6. SEM micrograph of a Si(400) membrane cross section showing a part of the γ-Al_2O_3 layer and the silica layer at high magnification (a) and the α-Al_2O_3 support and g γ-Al_2O_3 layers at lower magnification (b).

2.5.1.2 Gas Permeance

Permeance through microporous amorphous silica membranes occurs by solid-state-type diffusion of molecules. The permeance flux can be derived from Fick's First Law.
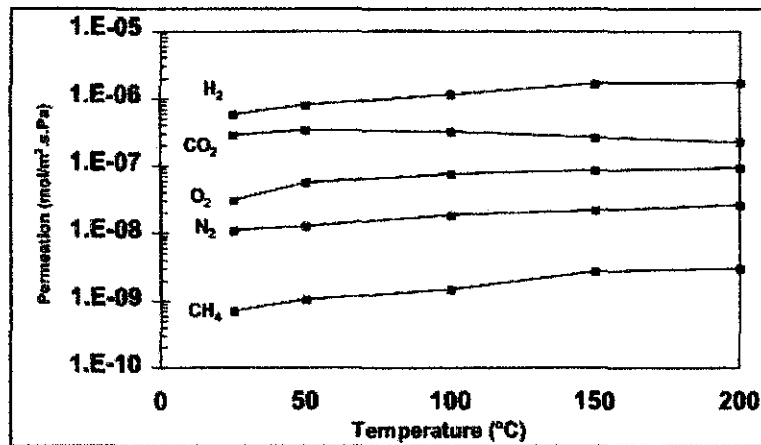
18

Fig. 2.7;Temp. dependence of the permeance for the Si(400) membranes at P=1 bar

Renate M. de Vos, Henk Verweij managed to produced Si(400) membranes that have a homogeneous 30 nm thick silica layer, which results in high permeances, e.g. for H_2 2×10^{-6}mol/m^2 s Pa at 200°C. They also show good permselectivities and separation factors, H_2/CH_4.The graph show that CH_4 have lowest permeance at all temperature thus give high permselectivity especially for H_2/CH_4 and CO_2/CH_4.

2.5.2 By Ruldolph et al.

Produced and synthesised a range of membrane that differ by their layering characteristic whether it is a "single step membrane" (noted as S) or "two step membrane" (noted as K) that describe these membrane are produced by single and two step catalysed hydrolysis sol-gel process respectively. These silica membranes are coated on α-alumina support substrate with 2 cm thick and average porosity of 30%.The deposition of membrane is achieved by dip coating method on the porous alumina support. The membrane was calcined at temperature between 400-600°C.

2.5.2.1 Gas Permeance

The gas permeation of those membranes was measure for a range of pressure and temperature.

19
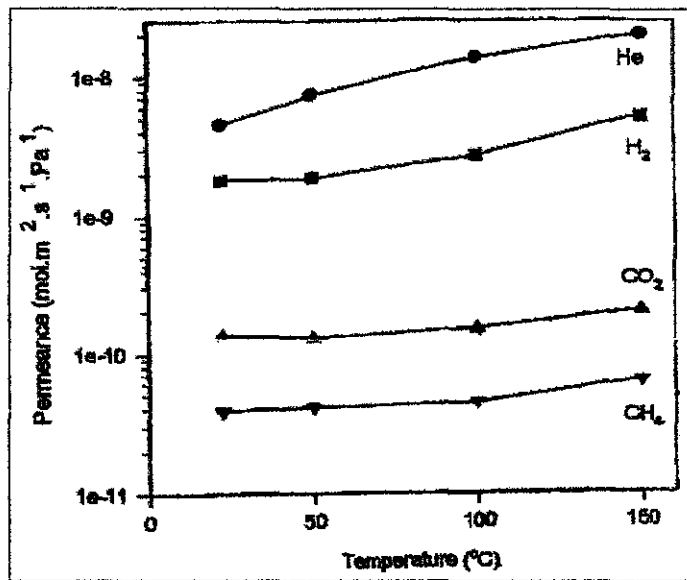
(a)
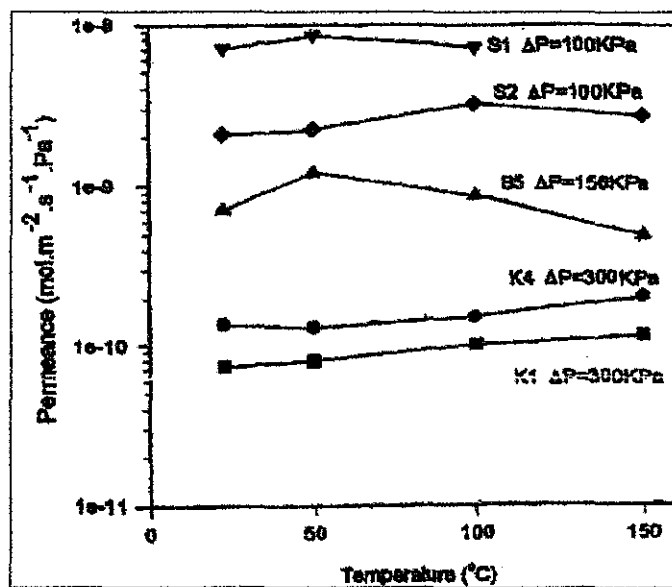
(b)

Fig 2.8; (a) Permeance of single-step membrane to various gases, (b) Comparison of permeance of Single and two step membrane to CO_2 as a function of temperature.

From Fig. 2.8(a) Ruldolph managed to established the general trend for gases with molecular kinetic diameter $d_k < 3$ Å and higher permselectivity for the gases with dk > 3 Å.Regarding Fig. 2.8(b) the significant difference between the single and two step membrane is that the permeance of the two step membrane for CO_2 is an order of magnitude lower. Therefore, Ruldolph have conclude that the two-step membrane process produced films that have better pore size control for pores size less than 3.4 Å. The results also show that CH_4 have lowest permeance at all temperature range thus give the possibility for separation of CO_2/CH_4.

CHAPTER 3
METHODOLOGY

3.1 Silica Membrane supported on porous alumina

There are two major component in this silica membrane which are Porous Alumina support that used as a support substrate for silica sol (silica membrane) and silica sol-gel itself. Therefore, there will be 2 stages of membrane synthesis which are:

1. Preparation of porous Alumina Membrane Support
2. Synthesis of the coating gel (silica sol).

3.2 Membrane Synthesis

3.2.1 Synthesis of Porous Alumina Support

Porous alumina, α-Al_2O_3 supports are made from alumina powder. The supports are pressed at 205-245 kPa, and sintering at 1500oC for 4 hours. The final porosity was 20 – 22 % determined using method base on the displacement of water into the substrate.

Experiment: Preparation of porous alumina support using extrusion method

The materials used for the support are aluminium oxide powder, starch and distilled water. Starch is used as a binder in developing porous alumina substrate. Methodology:

1. First, 100 mL beaker was filled with distilled water and boiled until 100^0C.
2. Then, dissolved 10 gram of starch into the 100ml boiled water.
3. Check the viscosity of the starch solution and if the solution is not adhesive enough add some starch till it become sticky.
4. After that, cool the solution to room temperature.
5. Then, 10 gram of aluminium oxide was prepared on the glass plate.

6. Then the solution of starch and distilled water was mixed with aluminium oxide powder using dropper and quickly pour the powder into a die press and press using handpress at 20 kPa – 24 kPa.

8. Steps 5 to 6 are repeated until we get a perfect alumina disc.

9. Then, the alumina discs were sintered at temperature between 1400°C to 1500°C in the furnace for 3 to 4 hours.

(a)   (b)   (c)
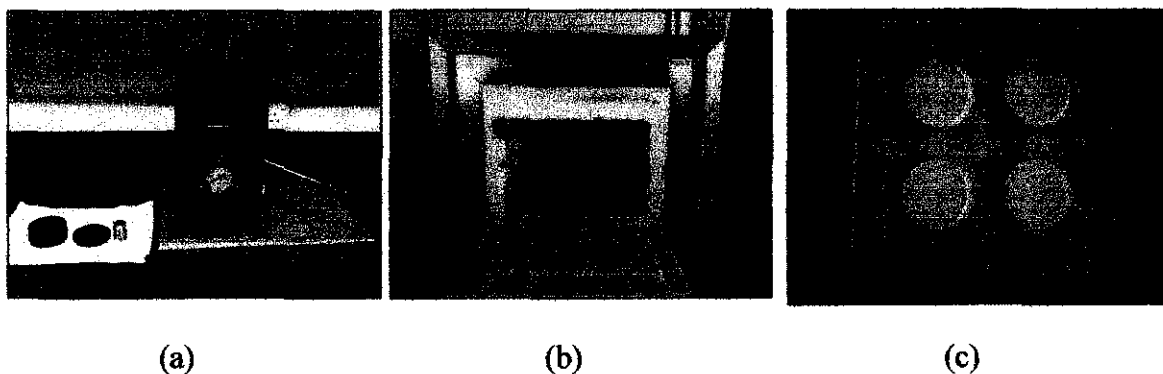
Figure 3.1; (a) Extrusion die and hand press used in Extrusion of Alumina powder to from porous alumina disc. (b) Furnace used in sintering process and (c) Sintered porous alumina membrane support.

3.2.2 Synthesis of Silica Sol-gel

Sol–gel silica was prepared by base catalysis of TEOS (Aldrich) and distilled water, with ethanol used as solvent. As catalysts, ammonium solutions (NH4OH) were used. Samples prepared in three groups [3]:

Group A: 2.76 ml TEOS solution were prepared together with 22.24 ml Ethanol (C_2H_5OH) in the 50 ml beaker.

Group B: 0.074 ml of ammonia solution (NH4OH) together with 24.92 ml ethanol (C_2H_5OH) in 50 ml beaker.

Group C: 6.3 ml distilled water and 18.7 ml ethanol (C_2H_5OH) were add into 50 ml beaker.

All sample prepared in each group was mixed together into 100 ml beaker. The silica sol samples produced then were aged at room temperature for 48 hours.

3.2.3 Silica Membrane Preparation

Silica membranes are prepared by dip-coating a prepared porous alumina support in a polymeric silica sol made by base-catalyzed hydrolysis and condensation of tetraethyl orthosilicate (TEOS), $Si(OCH_2CH_3)_4$, in ethanol as mention in section **3.2.2 Synthesis of Silica Sol-gel** .The supports were dipped in the sol in a vertical position, maintained submerged for 1hour, 2hour and 3hour,thus three sample with different dipping time have been prepared. After withdrawal, the membranes were dried for 30 min inside the oven at temperature $100^{\circ}C$ and after drying, they were calcined for 3 hour at $450-500^{\circ}C$.These whole process is repeated with exact parameter or condition but with different dipping time or submerging time of 2 and 3 hours.
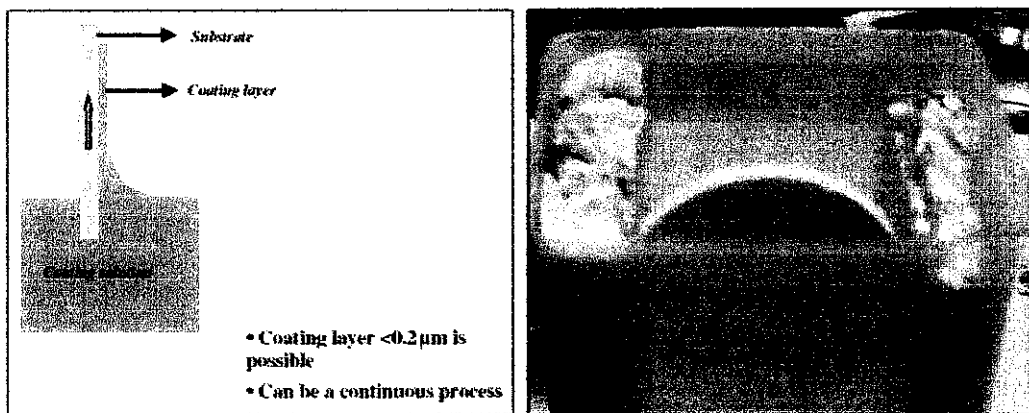

Figure 3.2; Dip-coating Method of the porous alumina support in silica sol

3.3 Membrane Characterization

Characterization techniques for silica membrane can be classified according to the nature of obtained parameter:

1. Morphology or structure related parameter
2. Permeation related parameter

Therefore, characterization techniques such as **Scanning Electron Microscope (SEM)** that will discussed for morphology/structure related parameter. While for the

permeation related parameter, characterization technique through **Permeation Test** (Permeability Test) is used.

3.3.1 Scanning Electron Microscope (SEM)

Scanning electron microscopy was used to characterize the structure of surface and sub-layer of membrane. Images obtained from SEM shows detailed 3-dimensional at much higher magnifications than is possible with a light microscope. Magnification of images is created by electrons instead of light waves as in conventional light microscope, which uses a series of glass lenses to bend the light waves.
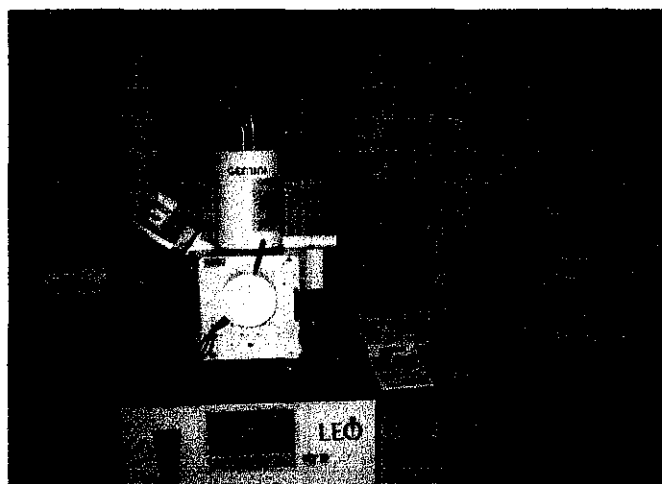

Figure 3.3; SEM for membrane morphology observation.

3.3.2 Gas Permeation Test

Gas permeation measurements were performed using pure CO_2 and pure CH_4. The permeation experiments flow single gas component of Carbon dioxide (CO_2) and methane (CH_4) through membrane disc. Feed side pressure was varied from 1.5 to 3 bar. The equipment set-up as illustrated in Figure 3.4 was used to carry out the gas permeation measurement. The set-up consists of a feed gas tank, a pressure gauge of inlet gas, a dead-end membrane cell and a bubble soap flow meter. Membranes were located in the dead end membrane cell or module. This type of module allows the feed gas to flow into the membrane perpendicularly to the membrane position.

Before performing the experiment, the gas permeation test unit was evacuated to less than 0.1 bar by vacuum pump for 1 hour to remove all residual gases remaining in the equipment. The feed gas was supplied directly from the gas tank, which is equipped with a pressure regulator. The feed gas pressure was set up within range of test pressure and the permeate stream was assumed to be at atmospheric pressure. In this permeation experiment, time (t) required to reach certain volume of gas in the permeate stream was observed and recorded. In addition, the volume of gas (V) in permeate stream was also measured using a bubble soap flow meter. The permeation of each gas through a membrane was measured twice at steady state condition.

Based on the volumetric measurements of the permeated gas, the volumetric flow rate Q, was calculated as follows:

$$Q = \frac{V}{t}$$ (3.1)

This volumetric flow rate was then corrected to STP conditions ($0^{o}C$ and 1 atm) using the following equation:

$$Q_{STP} = \frac{T_{STP}}{T} \times Q$$ (3.2)

in which T_{STP} and Q_{STP} referred to temperature (K) and volumetric of permeate gas (cm^3/s) at STP condition. After conversion into STP condition, gas permeance, P, was then calculated using the following formula

$$P = \frac{Nt}{A\Delta p}$$ (3.3)

where Δp and A were trans-membrane pressure and effective membrane area, respectively. Nt is the gas permeation rate (mol/s) and can be calculated as follows:

25

$$Nt = \frac{Q_{STP} \, x \rho_{CO2}}{M_{CO2}} \qquad (3.4)$$

where ρ_{CO2} and M_{CO2} were CO₂ density and molecular weight of CO_2, respectively. The CO_2/CH_4 ideal selectivity (unitless), α_{CO_2/CH_4}, of membrane can be determined by dividing CO_2 permeance, $(P)_{CO2}$, over CH_4 permeance, $(P)_{CH4}$.

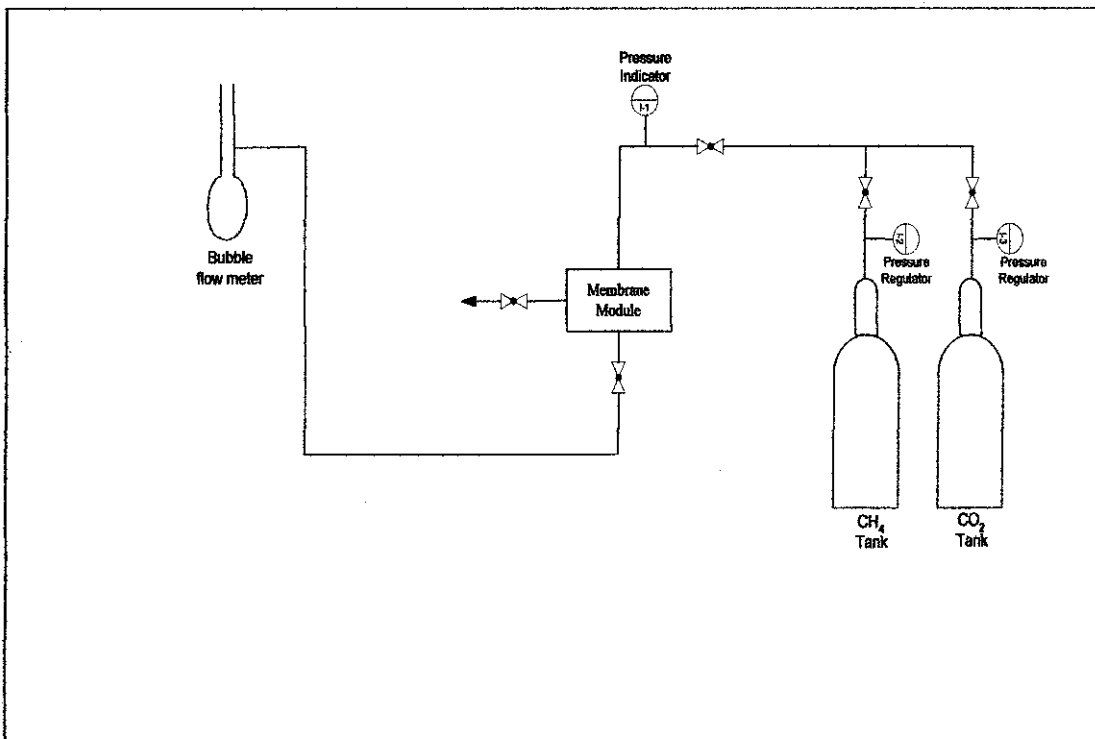$$\alpha_{CO_2/CH_4} = \frac{(P)_{CO_2}}{(P)_{CH_4}} \qquad (3.5)$$

Figure 3.4 Schematic diagram for membrane permeation studies.

CHAPTER 4

RESULT AND DISCUSSION

4.1 Morphological characterization of silica membrane

Surface morphology and cross-sections of membranes were studied by SEM. Figure 4.1 (a), (c), (d) show the top-view of the silica membrane with different dipping time of 1hour,2hour and 3 hour. These figures indicate the discrete layer of silica is successfully formed on top of porous alumina support. While, Figure 4.1 (b), (d), (f) show the cross-section view of the silica membranes which indicate clearly the silica layer deposited on top of the porous alumina support layer as a distinct separation between the two layers present.

Indeed, the skin layer was formed successfully. From the SEM observation, the surface of the support was covered with a continuous layer of silica particles and its' grew within the pores of the support. The silica membrane was tightly attached to the substrate and the thickness of the membrane varies from 9-15 μm. From these figure it show that the thickness of silica membrane is proportional to the dipping time.

This method has been shown to be very effective for the formation of mesoporous silica membranes on a support with relatively large pores.
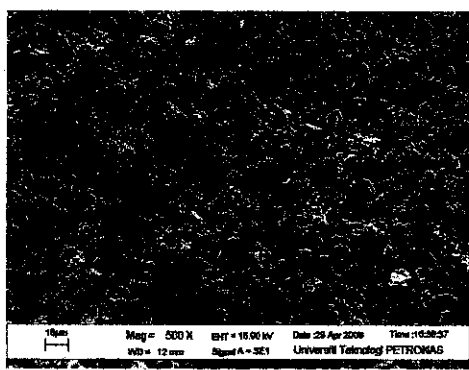
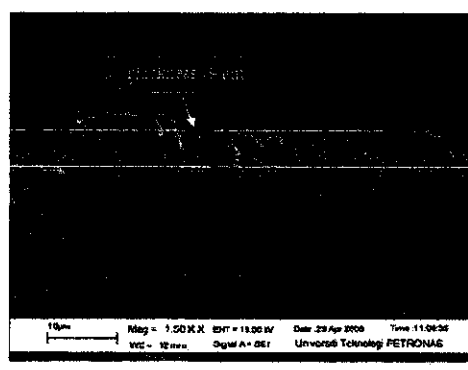Figure 4.1 (a) – Top view of silica membrane for 1 hour dipping time

Figure 4.1(b) – Cross-section view of silica membrane for 1 hour dipping time.
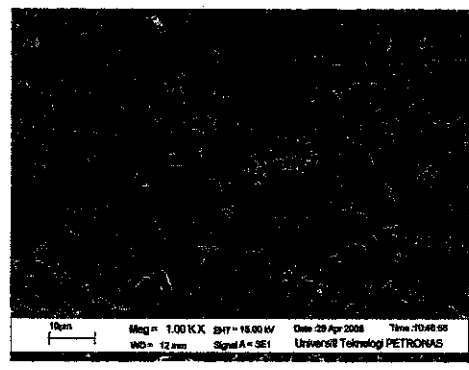

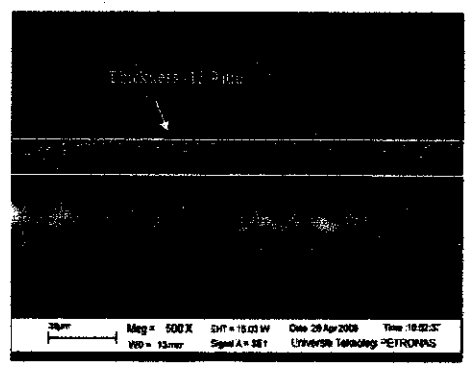Figure 4.1 (c) – Top view of silica membrane for 2 hour dipping time

Figure 4.1(d) – Cross-section view of silica membrane for 2 hour dipping time.
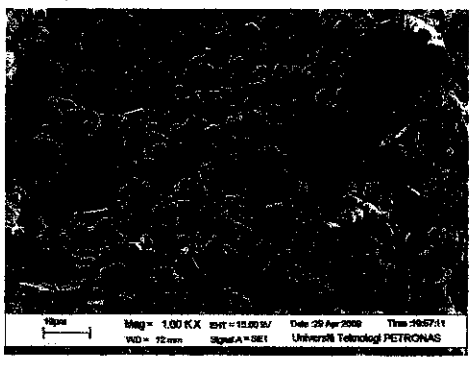

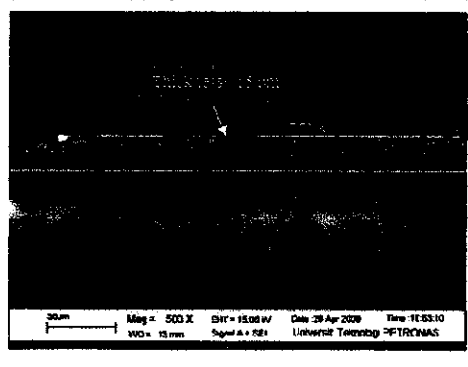Figure 4.1 (e) – Top view of silica membrane for 3 hour dipping time

Figure 4.1(f) – Cross-section view of silica membrane for 3 hour dipping time.

4.2 Gas Permeation

A permeation test through the samples was carried out using single component gas of Carbon dioxide (CO_2) and methane (CH_4). In mesoporous membranes, at pressures below (10 bar) 1×10^5 Pa, the permeation flux of a gas species is completely determined by Knudsen flow [33].

Table 4.1; Gas Permeation result for 1hour of dipping time

Applied Pressure (kPa)	Permeance Result (mol/m2.s.Pa)		Permeance As Ideal Selectivity
	CO_2	CH_4	CO_2/CH_4
150	2.82281E-06	2.42705E-06	1.163
200	3.16313E-06	2.6564E-06	1.191
250	3.6069E-06	3.11577E-06	1.158
300	4.12148E-06	3.36922E-06	1.223

Figure 4.2; CH_4 and CO_2 permeation versus pressure 1hour of dipping time

Table 4.2; Gas Permeation result for 2 hour of dipping time

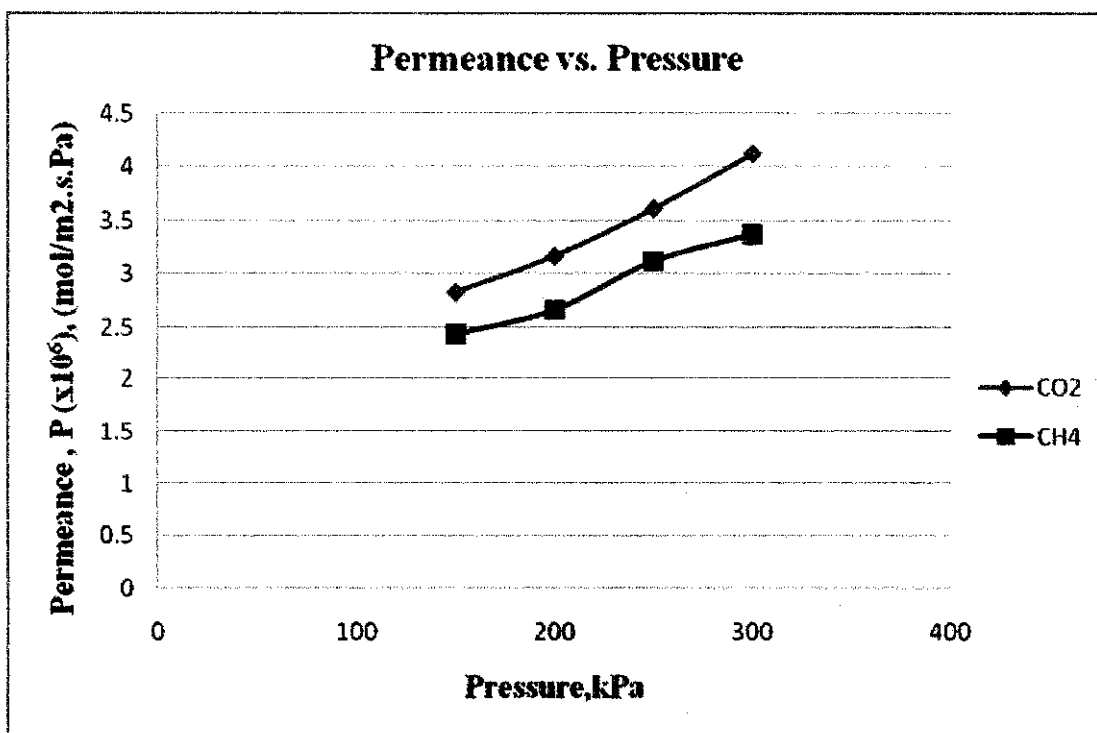| Pressure (kPa)	Permeance result (mol/m2.s.Pa)		Permeance result Ratio(CO2/CH4)
	CO2	CH4	
150	2.75129E-06	2.14275E-06	1.284
200	3.07613E-06	2.37173E-06	1.297
250	3.40572E-06	2.57035E-06	1.325
300	3.89317E-06	2.81909E-06	1.381
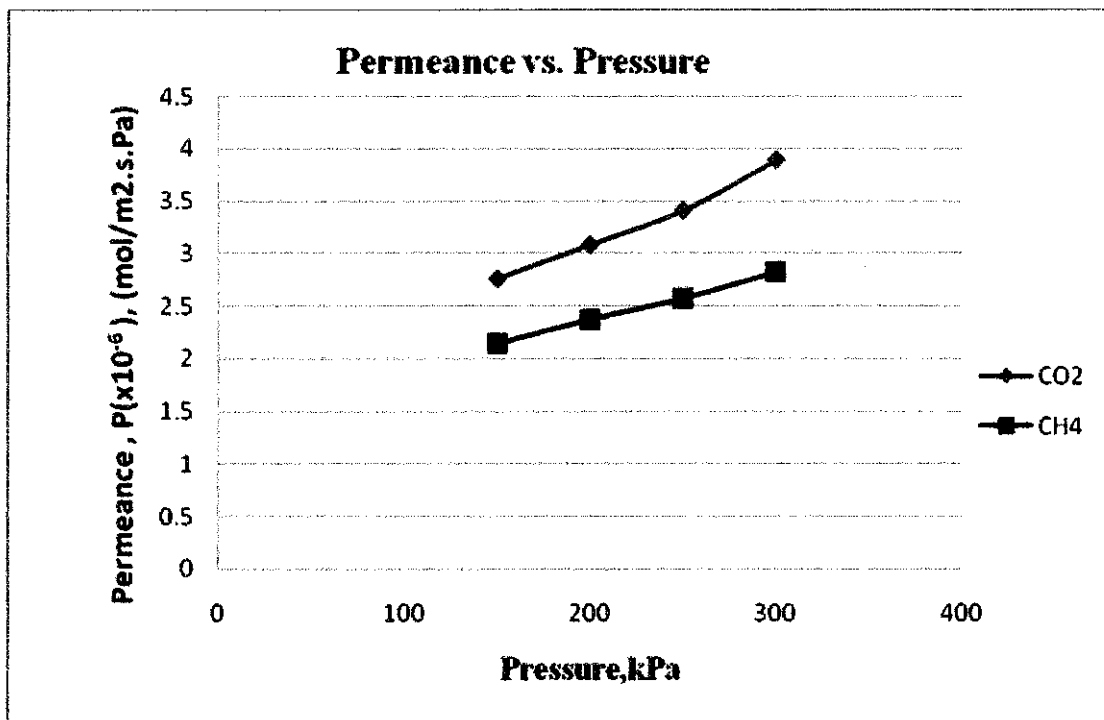
Figure 4.3; CH$_4$ and CO$_2$ permeation versus pressure for 2 hour of dipping time

Table 4.3; Gas Permeation result for 3 hour of dipping time

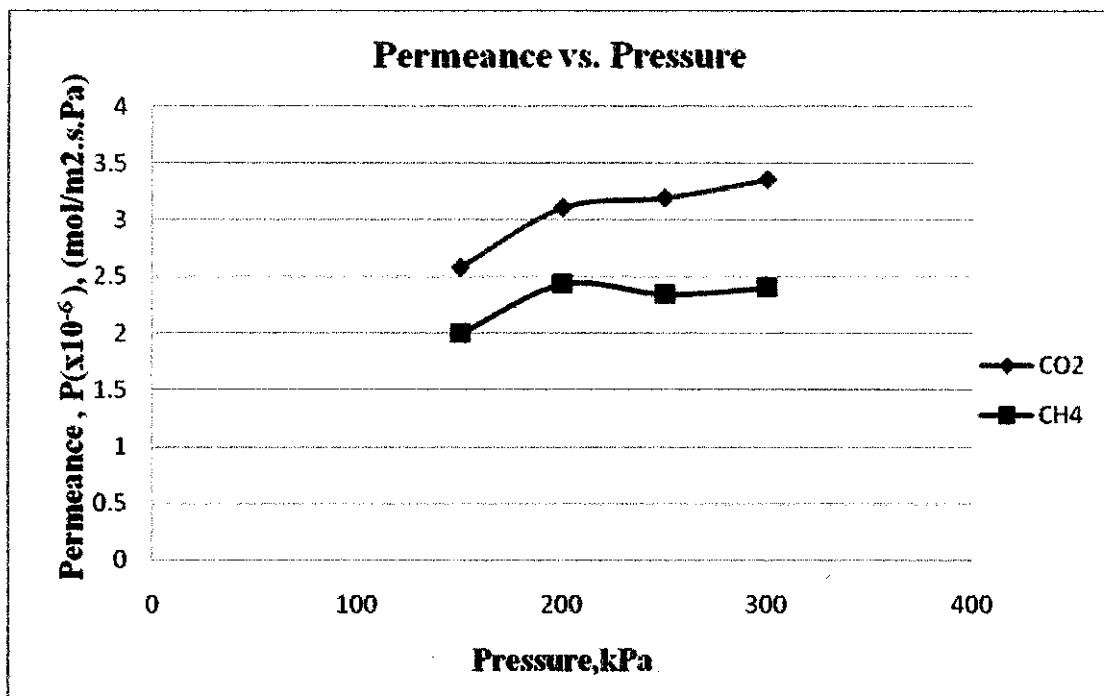|			
150	2.58352E-06	1.99808E-06	1.293
200	3.10985E-06	2.43719E-06	1.276
250	3.19572E-06	2.34634E-06	1.362
300	3.35963E-06	2.40317E-06	1.398

Figure 4.4; CH_4 and CO_2 permeation versus pressure for 3 hour of dipping time

Based on the result obtained, the permeance of the $CO_2 > CH_4$ for all synthesized silica membrane, thus give the evidence that the mechanism of molecular differentiation by silica layer is through size selectivity. The highest permselectivity obtained by the silica membrane with 1hour, 2hour and 3 houris dipping time are 1.223, 1.381 and 1.398 respectively. The result shows that the selectivity can be improved by controlling the dipping time so that optimal pore size and interconnected pore structure will be formed on the alumina porous support. Silica membranes with 3 hour dipping time result in good CO_2 permeance of 3.36×10^{-6} mol/m^2.s.Pa with maximum permselectivity of 1.398.

The ideal Knudsen separation factor is the ratio of the square roots of the molecular weight of each species. The ideal Knudsen separation factor for CO_2 over CH_4 is 1.66. In this study, the maximum separation factor of 1.398 is obtained at ΔP of 300 kPa for CO_2/CH_4 separation. Obviously this separation factor is slightly lower than Knudsen. This small deviation from ideal Knudsen diffusion may be due to a minute number of microcracks in the membrane layer, which were not observable by SEM, but detected by this test. Small defects and cracks often appear in thin films during the calcination process. These defects can often be repaired by repeating the synthesis process.

The separation factor for CO_2/CH_4 obtained using synthesized silica membrane which is 1.22 is smaller compared to other silica membrane produce by previous researcher. **Ruldolph et al.** managed to synthesize a high quality silica membrane that utilized nitric acid as a catalyst in hydrolysis process. All membrane produced have greater separation factor than the corresponding ideal Knudsen Diffusion separation factor especially for CO_2/CH_4. The separation factor for CO_2/CH_4 obtained by **Ruldolph et al.** was between 1.5 - 130 through their single and two step catalysed silica membranes.

The selectivity of the synthesized silica membrane can be improved through some modification which is by applying multiple separation layer of silica sol on the top or surface of the original silica coated membrane. This multiple separation layer can be done through sequences of dipping-drying-calcination step. In other words the membrane will be dipped in the silica sol, then dry before being calcined at desired

calcination temperature. Those steps will be repeated several times prior to get several separation layers on the membrane. It is found that, the selectivity of the membrane will be increased with an increase in the number of modified layer (M. Naito et. al, 1997).This can be explained by the self-repairing of the defect or microcracks existing in the previous formed separation layer of the silica membrane. This method of the formation of several separation layers will gradually decreased the pore size of the membrane leading to greater selectivity of separation gas especially CO_2 and CH_4 separation.

4.3 X-ray diffraction (XRD)
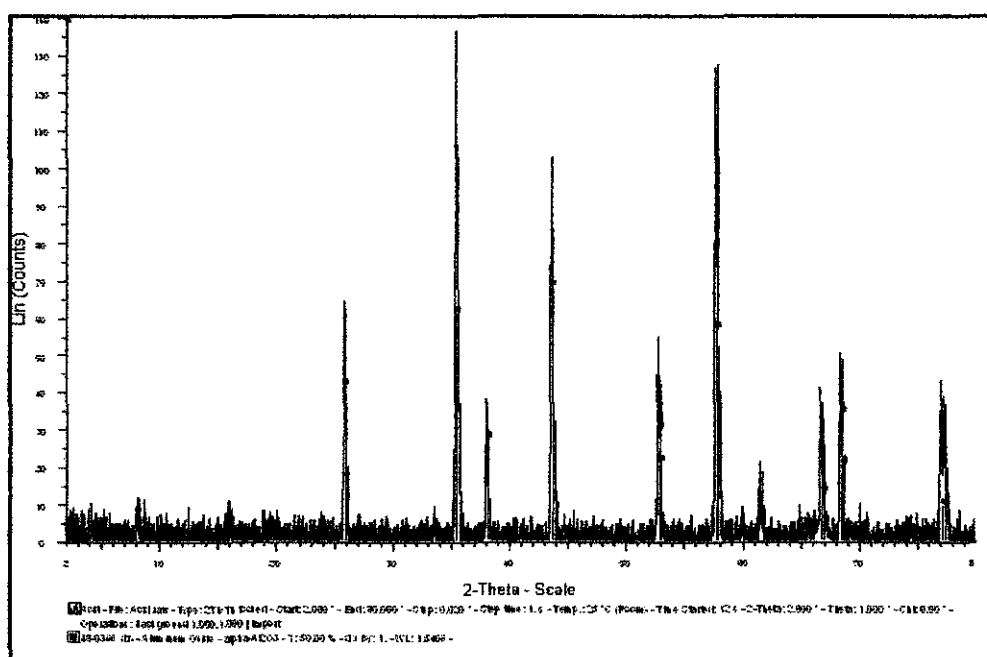
Figure 4.5; XRD pattern of samples calcined at 450-500°C.

In order to study the structure of silica membranes on porous alumina support, the membrane in powder form is directly characterized by XRD. Figure 4.5 shows the XRD pattern of membranes (powder) calcined at 450-500°C for 3 hours. The sharp peaks in the range of wide-angle XRD correspond to the characteristic peaks of α-Al2O3. Those sharp diffraction peaks clearly indicated that the powders possess a periodic mesostructure.

CHAPTER 5

CONCLUSION AND RECOMMENDATION

5.1 Conclusion and Recommendation

Silica membranes are successfully prepared through dip-coating a prepared porous alumina support in a polymeric silica sol made by base-catalysed hydrolysis and condensation of tetraethyl orthosilicate (TEOS), $Si(OCH2CH3)4$, in ethanol. The membranes were characterized using SEM and single gas permeability test. Silica membrane prepared via base-catalyst hydrolysis have successfully shown it's ability in separating CO_2 and CH_4 through the permeance of each gas, where the permeance of CO_2 gas are greater than permeance of CH_4 gas throughout all synthesized silica membranes in this study. This gives evidence that the mechanism of molecular differentiation by silica layer is through size selectivity.

The silica membranes managed to separate CO_2/CH_4 with a significant permeance value for both CO_2 and CH_4 (CO_2permeance > CH_4permeance) but with poor permselectivity of CO_2 over CH_4. This is may due to the formation of microcrack or defect during calcination process. The selectivity can be improved through modification of the silica membrane by applying multiple separation layers on the porous alumina support by sequences of dipping-drying-calcination step.

The dipping time can be considered important in silica membrane preparation because it will give the optimal pore size and interconnected pore structure on the alumina porous support. The longer the dipping time, better pore size control and finer interconnected pore structure of silica layer on the alumina support.

APPENDIX

Appendix A

Sample calculation for gas permeance: CO_2 permeance for dipping time of 1hour.

Pressure (bar)	Volume (cm3)	Time (s)						
1.500	50.000	3.430	14.577	13.490	0.687	0.00083160	0.00002823	2.82281E-06
2.000	50.000	3.070	16.287	15.072	0.767	0.00124248	0.00003163	3.16313E-06
2.500	50.000	2.700	18.519	17.137	0.873	0.00177099	0.00003607	3.6069E-06
3.000	50.000	2.370	21.097	19.524	0.994	0.00242837	0.00004121	4.12148E-06

Data:

$A = 19.64 \ cm^2$

MW $CO_2 = 44.01$

Pressure (bar)	CO_2		PCO_2	CH_4
1	1.804	0.6552	0.001804	0.000655
1.5	2.713	0.984	0.002713	0.000984
2	3.628	1.313	0.003628	0.001313
2.5	4.548	1.644	0.004548	0.001644
3	5.474	1.975	0.005474	0.001975
3.5	6.405	2.306	0.006405	0.002306

Based on the volumetric measurements of the permeated gas, the volumetric flow rate Q, was calculated as follows:

$$Q = \frac{V}{t}$$

$$Q = \frac{50 \ cm^3}{3.43 \ s}$$

$$Q = 14.577 \ cm^3 / s$$

This volumetric flow rate was then corrected to STP conditions ($0^{\circ}C$ and 1 atm) using the following equation:

$$Q_{STP} = \frac{T_{STP}}{T} \times Q$$

$$Q_{STP} = \frac{273K}{295K} \times 14.577$$

$$Q_{STP} = 13.49 cm^3 / s$$

After conversion into STP condition, gas permeance, P, was then calculated using the following formula

$$P = \frac{Nt}{A\Delta p}$$

where Δp and A were trans-membrane pressure and effective membrane area, respectively. Nt is the gas permeation rate (mol/s) and can be calculated as follows:

$$Nt = \frac{Q_{STP} x \rho_{CO2}}{M_{CO2}}$$

where ρ_{CO2} and M_{CO2} were CO_2 density and molecular weight of CO_2, respectively.

$$Nt = \frac{13.49 x 0.002713}{44.01}$$

$$Nt = 0.00083160 mol / s$$

$$P_{CO_2} = \frac{0.00083160}{(19.64)(1.5)}$$

$$P_{CO_2} = 2.823 x 10^{-5} mol / cm^2 .s.bar$$

$$P_{CO_2} = 2.823 x 10^{-6} mol / m^2 .s.Pa$$

The CO_2/CH_4 ideal selectivity (unitless), α_{CO_2/CH_4}, of membrane can be determined by dividing CO_2 permeance, $(P)_{CO2}$, over CH_4 permeance, $(P)_{CH4}$.

$$\alpha_{CO_2/CH_4} = \frac{(P)_{CO_2}}{(P)_{CH_4}}$$

REFERENCES

[1] R.W. Baker, Future directions of membrane gas separation technology, Ind. Eng. Chem. Res. 41 (2002) 1393.

[2] E.S. Sanders, BCFD-scale Membrane Separation Systems for CO2 Removal Application in Oil and Gas Production, submitted for publication.

[3] W.J. Koros, R. Mahajan, Pushing the limits on possibilities for large scale gas separation: which strategies? J. Membr. Sci. 175 (2000) 181.

[4] Y.S. Lin, Microporous and dense inorganic membranes: current status and prospective, Sep. Purif. Technol. 25 (2001) 39.

[5] J. Caro, M. Noack, P. Koelsch, R. Schaefer, Zeolite membranes, state of their development and perspective, Microporous Mesoporous Mater. 38 (2000) 3.

[6] R. Lai, G.R. Gavalas, ZSM-5 membrane synthesis with organic-free mixtures, Microporous Mesoporous Mater. 38 (2000) 239.

[7] K. Kusakabe, T. Kuroda, S. Morooka, Separation of carbon dioxide from nitrogen using ion-exchanged faujasite-type zeolite membranes formed on porous support tubes, J. Membr. Sci. 148 (1998) 13.

[8] J. Coronas, R.D. Noble, J.L. Falconer, Separations of C_4 and C_6 isomers in ZSM-5 tubular membranes, Ind. Eng. Chem. Res. 37 (1998) 166.

[9] G. Xomeritakis, Z. Lai, M. Tsapatsis, Separation of xylene isomer vapors with oriented MFI membranes made by seeded growth, Ind. Eng. Chem. Res. 40 (2001) 544.

[10] V. Nikolakis, G. Xomeritakis, A. Abibi, M. Dickson, M. Tsapatsis, D.G. Vlachos, Growth of faujasite-type zeolite membrane and its application in the separation of saturated/ unsaturated hydrocarbon mixtures, J. Membr. Sci. 184 (2001) 209.

[11] M. Kondo, M. Komori, H. Kita, K.-I. Okamoto, Tubular-type pervaporation module with zeolite NaA membrane, J. Membr. Sci. 133 (1997) 133.

[12] M.G. Sedigh, L. Xu, T.T. Tsotsis, M. Sahimi, Transport and morphological characteristics of polyetherimide-based carbon molecular sieve membranes, Ind. Eng. Chem. Res. 38 (1999) 3367.

[13] A.B. Fuertes, Preparation and characterization of adsorptionselective carbon membranes for gas separation, Adsorption 7 (2001) 117.)

[14] C.J. Brinker, T.L. Ward, R. Sehgal, N.K. Raman, S.L. Hietala, D.M. Smith, D.-W. Hua, T.J. Headley, Ultramicroporous silica-based supported inorganic membranes, J. Membr. Sci. 77 (1993) 165.

[15] C.J. Brinker, R. Sehgal, S.L. Hietala, R. Deshpande, D.M. Smith, D. Loy, C.S. Ashley, Sol–gel strategies for controlled porosity inorganic materials, J. Membr. Sci. 94 (1994) 85.

[16] R.M. de Vos, H. Verweij, Improved performance of silica membranes for gas separation, J. Membr. Sci. 143 (1998) 37.

[17] C.-Y. Tsai, S.-Y. Tam, Y. Lu, C.J. Brinker, Dual-layer asymmetric microporous silica membranes, J. Membr. Sci. 169 (2000) 255.

[18] "Teaching Chemistry; A Materials Science Companion", Eds. Ellis, A.B.; Geselbracht, M.J.; Johnson, B.J.; Lisensky, G.C.; Robinson, W.RT.; Ameican Chemical Society; 1993.]

[19] S.-T. Hwang, K. Kammermeyer, Can. J. Chem. Eng. 1996, 44, 82.

[20] A.B. Shelekhin, A.G. Dixon, Y.H. Ma, AIChE J. 1995, 41 (1), 58.

[21] A.J. Burggraaf, J. Membr. Sci. 1999, 155, 45.

[22] R.M. Barrer, J. Chem. Faraday Trans. 1990, 86 (7), 1123.

[23] J. Xiao, J. Wei, Chem. Eng. Sci. 1992, 47 (5), 1123.

[24] R.S.A. de Lange, K. Keizer, A.J. Burggraaf, J. Membr. Sci. 1995, 104, 81.

[25] V. Breger, E. Gileadi, Electrochim. Acta, 1971, 16, 177.

[26] M. Bhandarkar, A.B. Shelekhin, A.G. Dixon, Y.H. Ma, J. Membr. Sci. 1992, 75, 221.

[27] Y.H. Ma, Adsorption phenomena in membrane systems, in A.J. Burggraaf, L. Cot (Ed.),
Fundamentals of inorganic membrane science and technology, Elsevier, Amsterdam, 1996, pp. 36-42.

[28] I. Langmuir, J. Am. Chem. Soc. 1915, 37, 1139.

[29] M. Knudsen, Ann. Phys. 1909, 28, 75.

[30] J.S. Masaryk, R.M. Fulrath, *J. Chem. Phys.* **1973**, 59 (3), 1198.

[31] P.L. Studt, J.F. Shackelford, R.M. Fulrath, J. Appl. Phys. 1970, 41 (7), 2777.

[32] J.F. Shackelford, P.L. Studt, R.M. Fulrath, J. Appl. Phys. 1972, 43 (4), 1619.

[33] M. Mulder, Basic Principles of Membrane Technology, Kluwer Academic Publishers, Dordrecht, Netherlands (1991).